

1 **HIV-specific T-cell responses reflect substantive in vivo interactions with infected**  
2 **cells despite long-term therapy**

3  
4 **Authors and affiliations:**

5  
6 Eva M. Stevenson<sup>1#</sup>, Adam R. Ward<sup>1,2,3#</sup>, Ronald Truong<sup>2</sup>, Allison S. Thomas<sup>4</sup>, Szu-Han Huang<sup>1,2</sup>,  
7 Thomas R. Dilling<sup>1</sup>, Sandra Terry<sup>1</sup>, John K. Bui<sup>1</sup>, Talia M. Mota<sup>1</sup>, Ali Danesh<sup>1</sup>, Guinevere Q. Lee<sup>1</sup>,  
8 Andrea Gramatica<sup>1</sup>, Pragya Khadka<sup>1</sup>, Winiffer D. Conce Alberto<sup>1</sup>, Rajesh T. Gandhi<sup>5</sup>, Deborah K.  
9 McMahon<sup>6</sup>, Christina M. Lalama<sup>7</sup>, Ronald J. Bosch<sup>7</sup>, Bernard Macatangay<sup>6</sup>, Joshua C. Cyktor<sup>6</sup>,  
10 Joseph J. Eron<sup>8</sup>, John W. Mellors<sup>6</sup>, R. Brad Jones<sup>1,2\*</sup>, for the ACTG A5321 Team  
11  
12

13 <sup>1</sup>Division of Infectious Diseases, Weill Cornell Medicine, New York, NY USA

14 <sup>2</sup>Department of Microbiology, Immunology, and Tropical Medicine, George Washington  
15 University, Washington, DC USA

16 <sup>3</sup>PhD Program in Epidemiology, George Washington University, Washington, DC USA

17 <sup>4</sup>Department of Microbiology, Boston University School of Medicine, Boston, MA USA

18 <sup>5</sup>Division of Infectious Diseases, Massachusetts General Hospital, Boston, MA USA

19 <sup>6</sup>Department of Medicine, University of Pittsburgh School of Medicine, Pittsburgh, PA USA

20 <sup>7</sup>Center for Biostatistics in AIDS Research, Harvard T.H. Chan School of Public Health, Boston,  
21 MA USA

22 <sup>8</sup>Department of Medicine, University of North Carolina at Chapel Hill, Chapel Hill, NC USA  
23

24 #These authors contributed equally

25  
26 \*Corresponding author:

27 R. Brad Jones

28 [rbjones@med.cornell.edu](mailto:rbjones@med.cornell.edu)

29 413 E 69<sup>th</sup> St, 5<sup>th</sup> floor

30 New York, NY 10021  
31  
32  
33  
34  
35  
36  
37  
38  
39  
40  
41

42 **Abstract**

43 Antiretroviral therapies (ART) durably suppress HIV replication to undetectable levels – however,  
44 infection persists in the form of long-lived reservoirs of infected cells with integrated proviruses,  
45 that re-seed systemic replication if ART is interrupted. A central tenet of our current understanding  
46 of this persistence is that infected cells are shielded from immune recognition and elimination  
47 through a lack of antigen expression from proviruses. Efforts to cure HIV infection have therefore  
48 focused on reactivating latent proviruses to enable immune-mediated clearance, but these have  
49 yet to succeed in driving reductions in viral reservoirs. Here, we revisited the question of whether  
50 HIV reservoirs are predominately immunologically silent from a new angle, by querying the  
51 dynamics of HIV-specific T-cell responses over long-term ART for evidence of ongoing  
52 recognition of HIV-infected cells. We show that T-cell responses to autologous reservoir viruses  
53 persist over years, and that the maintenance of HIV-Nef-specific responses was uniquely  
54 associated with residual frequencies of infected cells. These responses disproportionately  
55 exhibited a cytotoxic, effector functional profile, indicative of recent *in vivo* recognition of HIV-  
56 infected cells. These results indicate substantial visibility of the HIV reservoir to T-cells on stable  
57 ART, presenting both opportunities and challenges for the development of therapeutic  
58 approaches to curing HIV infection.

59

60

61

62

63

64

65

66

67

## 68 Introduction

69 The needs for both a vaccine and a cure for HIV are underscored by the ongoing impact  
70 of this global pandemic, which continues to cause close to 800,000 deaths annually (1).  
71 Antiretroviral therapy (ART) is capable of durably suppressing HIV replication, and halting disease  
72 progression for those able to access and adhere to these regimens. Infection persists, however,  
73 in reservoirs of CD4<sup>+</sup> T-cells, and potentially other cell types (2, 3) with integrated proviruses that  
74 re-seed systemic replication if ART is interrupted (2, 4–9). These proviruses often exist in a latent  
75 state, characterized by limited transcription and, presumably, a lack of antigen production. This  
76 gives rise to one of the central tenets in the study of HIV persistence, which postulates that the  
77 persistent reservoir (often called the ‘latent reservoir’) is not detected by the immune system in  
78 individuals on long-term ART. It follows that engaging the immune system to reduce HIV  
79 reservoirs depends upon latency reversal to re-expose the immune system to HIV antigen – the  
80 so-called “kick and kill” (or “shock and kill”) strategy (10).

81 While latency undoubtedly diminishes immune recognition of viral reservoirs, several lines  
82 of evidence cast doubt on whether this is absolute *in vivo*, which would implicate additional  
83 contributors to viral persistence (11). Most notably, unspliced, and sometimes multiply spliced,  
84 HIV transcripts are readily detectable in peripheral blood mononuclear cells (PBMCs) of  
85 individuals on durable ART (12, 13). These observations have recently led some to propose  
86 amendments to the “latent reservoir” model, by introducing the idea of a continuum ranging from  
87 “deep latency” (no RNA produced) through to an “active reservoir” (14, 15). A key unresolved  
88 question, however, is whether these transcripts result in HIV-protein production, and thus enable  
89 immune recognition. Multiple factors limit the degree to which this can be inferred from direct  
90 measures of *in vivo* viral expression, including sampling difficulties – given that expression may  
91 be anatomically or temporally restricted – and the lack of equivalency between readily measurable

92 features (ex. viral RNA) with bonafide antigen presentation (16, 17). We therefore hypothesized  
93 that some level of antigen recognition by HIV-specific T-cells may occur *in vivo* in ART-  
94 suppressed individuals with undetectable viremia. We predicted that this would be reflected in  
95 relationships between the long-term dynamics of HIV-specific T-cell responses and measures of  
96 virologic persistence, including frequencies of infected cells.

97         Although the T-cell response to HIV infection has been generally well characterized, and  
98 is known to decay rapidly in the months following ARV initiation (18–20), there are a lack of well-  
99 powered studies that have addressed the long-term dynamics of these responses in association  
100 with virologic parameters. In a previous cross-sectional study, we observed a modest correlation  
101 between the magnitudes of T-cell responses to the HIV-Nef protein and residual frequencies of  
102 infected cells, providing some initial suggestion that these responses may be maintained by  
103 antigen recognition. However, a recent longitudinal study reported that, while responses were  
104 highly stable on durable ART, no correlations were observed between response magnitudes and  
105 reservoir size as measured by quantitative viral outgrowth assays across 18 individuals (21). The  
106 current study builds upon these earlier reports by uniquely assessing T-cell response dynamics  
107 over almost 3 years in association with multiple measures of viral persistence, in a cohort of 49  
108 individuals on well-documented sustained ART. We first confirm that, in this cohort, T-cell  
109 responses to autologous reservoir viruses are well represented by a scalable IFN- $\gamma$  enzyme-linked  
110 immunospot (ELISPOT) assay, and show that these responses persist over years. Strikingly, the  
111 persistence of T-cell responses to the HIV-Nef protein (slopes of change) over 144 weeks were  
112 strongly and uniquely associated with the frequencies of infected cells that persisted on ART (22,  
113 23), and these responses disproportionately exhibited a cytotoxic effector functional profile,  
114 indicative of recent *in vivo* antigen recognition (24–28). These results conclusively reveal ongoing  
115 interactions between the immune system and the HIV reservoir over years of ART, with

116 implications both for understanding HIV persistence, and designing interventions aimed at curing  
117 infection.

## 118 **Results**

### 119 *CD8<sup>+</sup> T-cell Responses to Autologous Infected Cells*

120 We approached the characterization of CD8<sup>+</sup> T-cell responses in our study with initial  
121 concerns over putative limitations in conventional approaches to quantifying T-cell responses to  
122 cells infected with autologous reservoir viruses. Namely, by utilizing synthetic peptides as  
123 antigens, conventional approaches may: i) detect responses from T-cells that are unable to  
124 recognize autologous reservoir viruses, as a result of sequence variation (13, 29); ii) not fully  
125 capture the entirety of viral epitopes, which may also be expressed from cryptic reading frames,  
126 or novel exon structures (23); and iii) skew representation of epitopes that are differentially  
127 affected by processing in infected cells (30).

128 With the aim of more comprehensively quantifying the total ability of CD8<sup>+</sup> T-cells to  
129 recognize infected cells, we developed a 'biosensor assay' whereby *ex vivo* CD8<sup>+</sup> T-cells were  
130 co-cultured with excess HIV-superinfected autologous CD4<sup>+</sup> T-cells. For each individual  
131 (participant characteristics in **Table S1**), we prepared two sets of target cells infected with either:  
132 i) the molecular clone of HIV, JRCSF, or ii) a cocktail of autologous reservoir viruses generated  
133 by pooling the supernatants of quantitative viral outgrowth assays (**Fig. 1A & B**). Flow cytometric  
134 analysis detected CD8<sup>+</sup> T-cells that responded to these infected cells by degranulating (CD107a)  
135 and/or producing IFN- $\gamma$ , in most individuals (**Fig. 1C**). In comparing these biosensor assay  
136 responses (to autologous viruses) with the total IFN- $\gamma$  ELISPOT responses (summed across all  
137 HIV gene products), we observed a strong correlation (Spearman  $r=0.840$ ,  $p=0.005$ , **Fig. 1D**), in  
138 spite of the above-noted putative limitations with using synthetic peptides. Thus, these data from  
139 our 'biosensor assay' serve to not only directly demonstrate that CD8<sup>+</sup> T-cell responses capable

140 of recognizing cells infected with autologous reservoir viruses remain present in individuals on  
141 long-term ART, but also to show that such responses are reasonably well represented by  
142 ELISPOT results, when summed across all HIV gene products.

### 143 *Magnitudes of T-cell Responses on Long-Term ART*

144 With the above validation in place, we leveraged the scalability of the ELISPOT assay to  
145 comprehensively examine T-cell response dynamics in a larger cohort. These assays were  
146 performed using overlapping 15-mer peptides spanning: i) HIV-Gag, ii) HIV-Env, iii) HIV-Pol, iv)  
147 HIV-Nef/Tat/Rev, v) HIV-Tat, vi) HIV-Rev, vii) HIV-Nef, and viii) CMVpp65 (control), with samples  
148 from the ACTG A5321 HIV Reservoirs Cohort Study, which consists of participants who initiated  
149 ART during chronic HIV infection and had subsequent well-documented, sustained virologic  
150 suppression (undetectable by clinical assay prior to and throughout the study period) (31) (**Fig. 2**  
151 **and Table 1**). We previously assessed HIV-specific T-cell responses in A5321 at study entry, a  
152 median of 7 (range 4-15) years after ART initiation (32). Here, we extended these results with  
153 batched analysis of samples from 24 and 168 weeks after study entry. IFN- $\gamma$ -producing HIV-  
154 specific T-cell responses were readily detected against Gag, Pol, and Nef, with median values at  
155 24 weeks: 103, 78.5, and 78.5 SFU/10<sup>6</sup> PBMCs, respectively; and at 168 weeks: 87.0, 44.7, and  
156 43.3 SFU/10<sup>6</sup> PBMCs, respectively (**Fig. 3A&B and Table S2**).

157 Between this 24 to 168 week period, time-averaged responses against Gag were the  
158 highest, and significantly greater than responses to Env, Nef, Tat, and Rev (all  $p < 0.05$ ) (**Table**  
159 **S3**). Notably, T-cell responses directed against Tat and Rev were the lowest in magnitude, and  
160 negligible at both timepoints (**Fig. 3B and Tables S2 & S3**), Env-specific responses were also  
161 low, with median values of 22.9 and 10.3 SFU/10<sup>6</sup> PBMCs at 24 and 168 weeks, respectively  
162 (**Fig. 3B and Table S2**). The long-term persistence of HIV-specific T-cell responses – primarily

163 directed against Gag, Pol, and Nef – over years of ART thus provided initial support for these  
164 HIV-specific T-cells continuing to interact with persisting infected cells.

#### 165 *Maintenance of Nef-Specific T-cells by the Reservoir*

166 To further characterize the long-term dynamics of HIV-specific T-cell responses in A5321  
167 cohort participants on durable ART, we categorized participants' IFN- $\gamma$  ELISPOT responses from  
168 the batched 24 to 168 weeks post-study entry data as either increasing, decreasing, or not  
169 changing (defined as  $\leq 15\%$  change), and observed considerable heterogeneity (**Fig. S1**).  
170 Notably, population-average responses to Nef, summed HIV, and CMV-pp65 did not decline  
171 significantly over this 144 week time period, whereas responses to Gag, Env, and Pol all showed  
172 significant declines over time (**Fig. 4A and Table S4**). However, all HIV-specific T-cell responses  
173 demonstrated remarkable persistence, with the responses which showed a significant decline  
174 only averaging between 0.35% to 0.62% loss per week in IFN- $\gamma$  ELISPOT assays (**Table S4**).

175 To determine whether ongoing antigen recognition by HIV-specific T-cells could be  
176 maintaining IFN- $\gamma$ -producing HIV-specific T-cell responses, we next examined associations  
177 between the slopes of change of T-cell response magnitudes between 24 and 168 weeks post-  
178 study entry (based on absolute changes on a linear scale) with on-ART virologic parameters,  
179 including total cell-associated HIV DNA (CA-DNA), cell-associated HIV RNA (CA-RNA), and  
180 plasma HIV RNA by integrase single copy assay (iSCA). The dynamics of responses to the most  
181 immunogenic antigens, Gag and Nef (33), along with summed HIV responses, were significantly  
182 associated with pre-ART viral loads (**Fig. 4B and Table S5**), despite participants having been on  
183 ART for over a median of 7 years when responses were first measured. Strikingly, however, the  
184 slopes of change in Nef-specific responses were unique in exhibiting highly significant direct  
185 associations with any on-ART virologic parameter after controlling for potential confounding by  
186 pre-ART plasma viral load and pre-ART CD4<sup>+</sup> T-cell count, specifically on-ART CA-DNA ( $r =$

187 0.496,  $p = 0.003$ ) and CA-RNA ( $r = 0.405$ ,  $p = 0.019$ ) at study entry (**Fig. 4B and Table S5**).  
188 These results indicate that both higher frequencies of persistent infected cells (CA-DNA) and  
189 higher levels of viral transcription (CA-RNA) were associated with greater maintenance of Nef-  
190 specific responses, consistent with ongoing stimulation by infected cells. Slopes of change in HIV-  
191 specific T-cell responses were not associated with PD-1 levels on total CD4<sup>+</sup> or CD8<sup>+</sup> T-cells (**Fig.**  
192 **4B and Table S5**), but generally correlated with each other (**Table S6**). Analyzing slopes of  
193 change in log<sub>10</sub>-transformed T-cell response magnitudes, reflecting proportional changes in  
194 responses rather than absolute changes, revealed significant associations between the dynamics  
195 of Nef-specific, Nef/Tat/Rev-specific, and summed HIV-specific T-cell responses with on-ART CA-  
196 DNA at study entry (all  $p < 0.05$  – **Table S7**), with proportional changes in HIV-specific responses  
197 generally correlating with each other (**Table S8**). Thus, whether dynamics were measured on an  
198 absolute or proportional change scale, Nef-specific response persistence was uniquely  
199 associated with HIV-infected cell frequencies. These results suggest that Nef-specific T-cell  
200 responses are preferentially maintained by ongoing interactions with HIV-infected cells, though  
201 all responses are likely maintained to some extent by ongoing HIV antigen recognition given their  
202 exceptional persistence.

### 203 *Recent In Vivo Antigen Recognition by Nef-Specific T-cells*

204 We next investigated whether the functional properties of HIV-specific CD8<sup>+</sup> T-cells would  
205 yield insights into their recent histories of *in vivo* antigen encounter. Data from human studies and  
206 animal models have highlighted *ex vivo* granzyme B production as a distinguishing feature of  
207 virus-specific effector CD8<sup>+</sup> T-cells which have recently encountered antigen *in vivo* - either  
208 through infection or vaccination (24–28). While granzyme B production can be induced in memory  
209 CD8<sup>+</sup> T-cells, this requires more than 24 hours of *in vitro* stimulation, whereas IFN- $\gamma$  is produced  
210 rapidly from both memory and effector CD8<sup>+</sup> T-cells (24, 34, 35). Thus, *ex vivo* ELISPOT  
211 measurements of granzyme B have been established as an ‘immune diagnostic’ means of



212 identifying effector responses to active infections (34, 36). To quantify the effector functionalities  
213 of HIV-specific T-cells on long-term ART, we performed batched granzyme B ELISPOT assays  
214 on week 24 and 168 samples (**Fig. 5A**). We focused on the Gag, Pol, and Nef peptide pools,  
215 having observed these to be the most immunogenic by IFN- $\gamma$  ELISPOT. Overall, granzyme B-  
216 producing HIV-specific responses were substantially lower in magnitude than IFN- $\gamma$  responses  
217 (**Fig. 5B, 5C and Table S2**). The median magnitudes of granzyme B responses relative to each  
218 other were: Nef>Pol>Gag (at both timepoints – **Fig. 5B and Table S2**), contrasting with IFN- $\gamma$ :  
219 Gag>Pol~Nef (**Fig. 3B and Table S2**). As with IFN- $\gamma$ , categorizing participants' granzyme B  
220 responses as either increasing, decreasing, or not changing revealed heterogeneity (**Fig. S2**),  
221 though proportionally there were fewer decreasing responses, and the population-average levels  
222 of granzyme B responses were highly stable over time to all HIV-gene products (**Fig. 5B and**  
223 **Table S4**). In contrast to IFN- $\gamma$ , we did not observe any significant correlations between the slopes  
224 of change of granzyme B responses with virologic measures of HIV persistence (**Tables S9 &**  
225 **S11**). These results may reflect the additional complexity that whereas both IFN- $\gamma$ - and granzyme  
226 B-producing cells can be maintained by infected cells producing antigen, the latter are more likely  
227 to also perturb the virologic measures by eliminating infected cells (37).

228 To further assess the functional profiles of HIV-specific T-cell responses, we performed  
229 pairwise comparisons of granzyme B versus IFN- $\gamma$  responses for each of the gene products tested  
230 (**Fig. 5C**). At both timepoints, granzyme B response magnitudes to Gag, Pol, and CMV-pp65 were  
231 substantially lower than IFN- $\gamma$  responses (all  $p < 0.05$ ) (**Fig. 5C**). Contrasting this, the magnitudes  
232 of granzyme B versus IFN- $\gamma$  responses to Nef were not significantly different from each other at  
233 either timepoint ( $p = 0.100$  at week 24,  $p = 0.277$  at week 168). These data indicate that in addition  
234 to being preferentially maintained over time, T-cell responses directed against the early HIV gene  
235 product Nef disproportionately exhibit effector functional profiles, as compared to the late gene  
236 products Gag and Pol (though appreciable granzyme B responses to these gene products were

237 still detected). Persistent HIV-specific granzyme B responses are indicative of recent antigen  
238 encounter, supporting the hypothesis that there is *in vivo* stimulation by HIV-infected cells despite  
239 suppressive ART.

## 240 **Discussion**

241 An important aspect of how HIV persists in individuals on long-term ART is through the  
242 evasion of immune recognition, predominately thought to be achieved through the maintenance  
243 of strict viral latency, with an additional aspect of anatomical sequestration. This perception that  
244 the reservoir is entirely latent has begun to shift lately, in response both to a new understanding  
245 of the dynamic nature of the HIV reservoir (driven by the clonal expansion of infected cells), and  
246 to new insights into ongoing viral transcriptional activity on ART (15, 38). To date, however, this  
247 has yet to prompt widespread re-consideration of the relationship between the HIV-specific T-cell  
248 response and the HIV reservoir. The current study provides evidence which challenges the  
249 prevailing model of a lack of reservoir immune surveillance, by indicating a level of ongoing  
250 antigenic stimulation of HIV-specific T-cells in ART-suppressed individuals. Nef-specific T-cells  
251 stood apart from those of other HIV gene products in this regard, supporting that early gene  
252 products (Nef, Tat, and Rev – of which only Nef was appreciably immunogenic [as also seen in  
253 other studies (21, 33)]) have lower thresholds to expression in a reactivation setting as compared  
254 to late gene products (Gag, Pol, and Env), which are expressed only after a cell has built up  
255 sufficient levels of Rev to drive nuclear export of unspliced and singly-spliced viral transcripts (39,  
256 40). The preferential maintenance of Nef-specific T-cells was presented as a hypothesis of the  
257 current study based, in part, on our previous observation that Nef-specific T-cells recognized cells  
258 reactivated from an *in vitro* latency model prior to recognition by Gag-specific T-cells, or  
259 detectable Gag expression (32).

260 Do our results allow for any inferences into how frequently infected cells are recognized  
261 by HIV-specific T-cells *in vivo*? While numerous aspects of complexity introduce caveats to such  
262 an analysis (e.g. tissue distributions), our data do allow for side-by-side comparisons between the  
263 peripheral blood frequencies of infected cells with antigen-expression potential, and those of HIV-  
264 specific T-cells – which may be informative. The median frequency of Nef-specific T-cells at week  
265 24 of our study was  $78.5/10^6$  PBMCs, whereas the median total frequency of HIV-infected cells  
266 (CA-DNA) was  $515.7/10^6$  CD4<sup>+</sup> T-cells (at week 0), or roughly  $103/10^6$  PBMCs. These infected  
267 cells, however, predominately contain defective proviruses (41), many of which are likely  
268 incapable of expressing antigens (42). It can therefore be reasonably estimated that, in most  
269 individuals, Nef-specific T-cells are at least as frequent as infected cells with the potential to  
270 express antigen. Our data indicating that the former are influenced by the latter therefore suggest  
271 that antigen expression is more likely to be a common versus a rare event *in vivo*, amongst  
272 infected cells with this potential. Further study is needed, however, and characterizing the clonal  
273 dynamics of HIV-specific T-cells may yield additional insights.

274 Although latency almost certainly contributes to viral persistence, our findings indicating that  
275 HIV reservoirs are not fully hidden from circulating cytotoxic T-cells raise the question of what  
276 additional mechanisms may be at play. We first consider the role of immune escape - the process  
277 by which HIV evades recognition by acquiring mutations in T-cell epitopes. Immune escape plays  
278 a critical role in limiting the overall efficacy of the HIV-specific T-cell response in untreated  
279 infection, and HIV reservoirs show clear evidence of past selection, in the form of extensive  
280 sequence variation in known T-cell epitopes (29). However, the question at hand pertains to HIV-  
281 specific T-cell responses that show evidence of being maintained by recent antigen recognition,  
282 indicating that they target epitopes which are intact in at least a portion of the reservoir. Further  
283 supporting this idea are the previous observations that: i) the fixation of escape mutations leads  
284 to the contraction of corresponding T-cell responses (43), and ii) the substantial majority of HIV-

285 specific T-cells that remain detectable after years of ART target epitopes for which escape is not  
286 fixed in corresponding reservoir viruses (44, 45). As with latency, our data do not lead us to  
287 contest the idea that the fixation of escape mutations in the reservoir diminishes the overall  
288 potential for immune recognition, nor the value of therapeutic strategies to address either of these  
289 limitations. However, we are still left with the question of how to reconcile our findings indicating  
290 an appreciable level of ongoing *in vivo* recognition of infected cells by cytotoxic (granzyme B) T-  
291 cells, with the overall stability of HIV reservoir sizes.

292 We therefore draw from two recent findings in the field to propose how an HIV reservoir may  
293 persist without being fully hidden from circulating cytotoxic T-cells. The first derives from the  
294 recent demonstrations that the HIV reservoir is predominately composed of infected T-cells that  
295 have undergone clonal expansion (46–48), with different clones dynamically ‘waxing and waning’  
296 over time (48). Thus, HIV-specific T-cells may frequently eliminate infected cells, only to have  
297 these replaced by clonal expansion of other reservoir-harboring cells. There have been somewhat  
298 conflicting recent reports regarding this possibility – from groups that approached the question  
299 from different angles - highlighting the need for further study (42, 49, 50).

300 Second, we have recently reported that reservoir-harboring cells exhibit intrinsic resistance  
301 to T-cell mediated elimination (51), mediated in part by BCL-2 over-expression, which  
302 antagonizes perforin/granzyme killing (52). In fact, while it has been generally assumed in our  
303 field that the encounter between an antigen-expressing HIV-infected cell and a functional (ex.  
304 perforin/granzyme releasing) CD8<sup>+</sup> T-cell will result in elimination, this overlooks the role of the  
305 target cell as an active partner in the killing process. Multiple regulatory mechanisms exist, both  
306 in physiological and pathological states, by which target cells determine whether or not to undergo  
307 apoptosis, despite receiving a perforin/granzyme hit (53, 54). Thus, one way to resolve our  
308 findings with others in the field is to propose that the recognition of HIV-infected cells by HIV-

309 specific cytotoxic T-cells may occur with some frequency *in vivo*, but that this often does not result  
310 in target cell elimination. An intriguing possibility is that the combined effects of selection, based  
311 on intrinsic susceptibility to CD8<sup>+</sup> T-cells, and clonal expansion of surviving cells may enable the  
312 evolution of a resistant reservoir, paralleling the phenomenon of ‘immunoediting’ in cancer (11).  
313 While latency reversal will likely be a critical component of curing HIV infection, our findings raise  
314 the hypothesis that – in lieu of an ideal latency reversing agent – reductions in HIV reservoirs may  
315 be achievable by boosting immune targeting of existing expression of early gene products (such  
316 as Nef, and in a manner that targets non-escaped epitopes,) while enhancing cytotoxic function,  
317 limiting clonal expansion, and addressing resistance to cytotoxic T-cells in reservoir-harboring  
318 cells.

## 319 **Methods**

### 320 *Study Design*

321 For these observational studies, we evaluated participants from two separate populations. The  
322 data in **Fig. 1** were collected on participants diagnosed with HIV infection recruited via  
323 convenience sampling through Maple Leaf Medical Clinic in Toronto, Canada. Outliers were not  
324 defined or excluded. Participants in this Toronto cohort were virally suppressed for a minimum of  
325 2 years prior to a leukapheresis procedure to collect PBMCs, with no reported ART interruptions  
326 or detectable viral loads by a commercial clinical assay. The objective of this first study was to  
327 evaluate the total ability of participant’s CD8<sup>+</sup> T-cells to recognize autologous HIV reservoir  
328 viruses, and to compare these results with T-cell responses as measured by IFN- $\gamma$  ELISPOT. All  
329 other data for this manuscript were collected on a longitudinal cohort of participants who initiated  
330 ART during chronic HIV infection in AIDS Clinical Trials Group (ACTG) trials for treatment-naïve  
331 individuals, and enrolled in the ACTG HIV Reservoirs Cohort Study (A5321) (31). A5321 cohort  
332 participants were recruited from 17 clinical research sites in the United States through the ACTG

333 network. IFN- $\gamma$  ELISPOTs were previously performed using samples from 96 participants at  
334 A5321 study entry (32), and a subset of 49 participants were selected from the original 96 for this  
335 longitudinal sub-study based on sample availability. All gene products and negative controls were  
336 tested in duplicate, with one replicate of PHA positive control. Assays performed under these  
337 same conditions have been previously validated in other participant cohorts. Outliers were not  
338 defined or excluded. Participants in the current sub-study had follow-up at least every 6 months  
339 following study entry, with documented sustained viral suppression (plasma HIV RNA levels <50  
340 copies/mL by commercial assays starting at week 48 on ART and at all subsequent timepoints –  
341 **Fig. 2**). One participant had a large viral blip (>1,000 copies/mL) 43 weeks prior to their 168 week  
342 A5321 study timepoint, and data was right-censored for this participant after the 24 week A5321  
343 study timepoint. Clinical data and paired plasma and PBMC samples were available from pre-  
344 ART and on ART study visits. We measured HIV levels (CA-DNA, CA-RNA, and plasma iSCA)  
345 and PD-1 levels (on CD4<sup>+</sup> and CD8<sup>+</sup> cells) on samples obtained at A5321 study entry (median 7  
346 years on ART), and plasma HIV RNA levels and CD4<sup>+</sup> T-cell counts were obtained from pre-ART  
347 clinical data. One participant later revoked consent for further testing and was excluded from  
348 analysis. We hypothesized *a priori* that the long-term dynamics of T-cell responses to the early  
349 HIV gene product Nef (measured by IFN- $\gamma$  ELISPOT) would be associated with infected cell  
350 frequencies.

### 351 *Virologic Assays*

352 HIV CA-DNA and CA-RNA were measured by quantitative PCR (qPCR) assays in PBMCs using  
353 previously described methods (55). CA-DNA and CA-RNA values per million CD4<sup>+</sup> T-cells were  
354 calculated by dividing the total CA-DNA or CA-RNA copies/million PBMCs (normalized for CCR5  
355 copies measured by qPCR as published (55)) by the CD4<sup>+</sup> T-cell percentage (x 0.01) reported  
356 from the same specimen date or from a CD4<sup>+</sup> T-cell percentage imputed using linear interpolation

357 from specimen dates before and after the CA-DNA or CA-RNA results. Cell-free HIV RNA was  
358 quantified by iSCA in blood plasma (5 mL) (56).

### 359 *Immunologic Assays*

360 PBMCs obtained at A5321 study entry were stained with the following monoclonal antibodies to  
361 evaluate surface PD-1 expression: CD3 APC-H7, CD4 PC5, CD8 V450, PD-1 (clone M1H4) A488  
362 (all from BD Biosciences, San Diego, California, USA), and Live/Dead Aqua (Invitrogen, Grand  
363 Island, New York, USA). Cells were fixed in 1% paraformaldehyde, and analyzed using a BD LSR  
364 Fortessa (FACSDiva) within 24 hours after staining. Lymphocytes were identified based upon size  
365 and granularity. The lymphocyte population was filtered through side scatter area vs. side scatter  
366 height histogram to eliminate doublets from the analysis. Single cells were analyzed using  
367 Live/Dead Aqua dye exclusion and then CD4<sup>+</sup> and CD8<sup>+</sup> populations were defined based on dual  
368 expression with CD3. These two populations were plotted against PD-1. Fluorescence minus one  
369 (FMO) controls were used to define the PD-1<sup>+</sup> T-cell populations.

### 370 *Quantitative Viral Outgrowth Assay (QVOA)*

371 Quantitative Viral Outgrowth Assays (QVOA) were performed as previously described (57).  
372 Briefly, CD4<sup>+</sup> T-cells were isolated from PBMCs by negative selection (Easysep, Stemcell  
373 Technologies) and plated in serial dilution at either 4 or 6 concentrations (12 wells/concentration,  
374 24-well plates). CD4<sup>+</sup> T-cells were stimulated with phytohemagglutinin (PHA, 2µg/mL) and  
375 irradiated allogeneic HIV-negative PBMCs were added to further induce viral reactivation. MOLT-  
376 4/CCR5 cells were added at 24 hours post-stimulation as targets for viral infection. Culture media  
377 [RPMI 1640 + 10% FBS + 1% Pen/Strep +50U/mL IL-2 + 10ng/mL IL-15 (R10-50-15)] was  
378 changed every 3 days and p24 enzyme-linked immunosorbent assay (ELISA, NCI Frederick) was  
379 run on day 14 to identify virus-positive wells. Infectious Units per Million CD4<sup>+</sup> T-cells (IUPM)  
380 values were determined using the Extreme Limiting Dilution Analysis (ELDA) software

381 (<http://bioinf.wehi.edu.au/software/elda/>) (58). Culture supernatants from virus-positive wells were  
382 frozen (-80°C) for future use.

### 383 *CD8<sup>+</sup> T-cell Biosensor Assay*

384 Activation of CD4<sup>+</sup> T-cell Targets: CD4<sup>+</sup> T-cells were enriched by negative selection (Easysep,  
385 Stemcell Technologies), typically starting from 200x10<sup>6</sup> PBMCs per study participant. These cells  
386 were stimulated with 10µg/ml of anti-CD3 (OKT-3) and anti-CD28 (28.2) antibodies (Ultra-LEAF™,  
387 Biolegend) in R10-50-15 for 48 hours. Infections: Cells were then washed, and split into 3 equal  
388 aliquots (~4x10<sup>6</sup> cells each) for infection with either: i) JRCSF ii) autologous virus or iii) mock  
389 (nothing). The autologous virus stock was generated by pooling equal volumes of all p24<sup>+</sup> QVOA  
390 wells from that study participant, while the JRCSF stock was generated by transfection of 293T  
391 cells with plasmid. All viruses were titrated on TZM-bl cells, and used at a MOI of 0.4. After a 2  
392 hour infection period at 37°C 5% CO<sub>2</sub>, cells were washed and then cultured for 48 hours in R10-  
393 50. Levels of infection were monitored every 24 hours by surface staining small aliquots with anti-  
394 CD3 Brilliant Violet 785™, CD4 Pacific Blue™ (Biolegend), then permeabilizing (BD  
395 Cytofix/Cytoperm™) and staining intracellularly with anti-HIV-Gag Kc57-RD1 (Beckman Coulter),  
396 and analyzed on a BD LSRFortessa™ flow cytometer. Infections were harvested for co-culture  
397 with CD8<sup>+</sup> T-cells, when they reached 2-4% Gag<sup>+</sup> within the CD3<sup>+</sup> gate.

398 Co-culture with CD8<sup>+</sup> T-cells: CD8<sup>+</sup> T-cells autologous to these CD4<sup>+</sup> targets were enriched on  
399 the day of co-culture from freshly a thawed aliquot of 100x10<sup>6</sup> PBMCs by negative selection  
400 (Easysep™, Stemcell Technologies). Infected and mock-infected CD4<sup>+</sup> T-cells were washed 5x  
401 and then co-cultured with CD8<sup>+</sup> T-cells at ratios of 5 CD8<sup>+</sup> T-cells to 1 CD4<sup>+</sup> T-cell, at a total  
402 concentration of 5x10<sup>6</sup> cells/mL in RPMI 1640 + 10% FBS + 1% Pen/Strep +50U/mL IL-2 (R10-  
403 50) with 1/100 anti-CD107a-PE antibody (Biolegend) and 1/1,000 Monensin GolgiStop™ (BD).  
404 Cells were incubated for a total of 6 hours, with mixing by pipetting every 30 minutes (to facilitate



405 contacts between antigen-specific CD8<sup>+</sup> cells and targets). Staining and Analysis: Cells were  
406 surface stained with anti-CD3 Brilliant Violet 785™, CD4 Pacific Blue™, CD8 Alexa Fluor® 700,  
407 and LIVE/DEAD™ Fixable Aqua dye (ThermoFisher). Cells were then washed, permeabilized (BD  
408 Cytofix/Cytoperm™), stained intracellularly with anti-HIV-Gag Kc57-RD1 (Beckman Coulter), and  
409 analyzed on a BD LSRFortessa™ flow cytometer.

#### 410 *Peptide Pools*

411 The following sets of consensus HIV clade B 15 amino acid peptides (overlapping by 11 amino  
412 acids) were supplied by the NIH AIDS Research and Reference Reagent Program: Gag (cat #  
413 8117), Env (cat # 9480), Pol (cat # 6208), Tat (cat # 5138), Rev (cat # 6445), and Nef (cat # 5189).  
414 All peptides were dissolved at 5mg/mL in 12.5% DMSO (Corning), and 87.5% PBS (Gibco).  
415 Peptides were pooled into whole gene product peptide pools and adjusted to a final concentration  
416 of 20µg/mL/peptide in PBS. A CMV-pp65 PepMix peptide pool (JPT Peptide Technologies) was  
417 dissolved separately in DMSO and adjusted to a final concentration of 20µg/mL/peptide in PBS.

#### 418 *IFN-γ and Granzyme B ELISPOT Assays*

419 Multi-screen IP 96-well PVDF plates (Millipore) were either directly coated with 100µL/well of PBS  
420 + 0.5µg/mL primary anti-human IFN-γ antibody (clone 1-D1K, Mabtech) overnight at 4°C, or first  
421 primed with 20µL of 35% EtOH/well, and immediately washed 6x with 200µL ddH<sub>2</sub>O and then  
422 coated with 100µL/well of PBS + 15µg/mL primary anti-human granzyme B antibody (clone GB10,  
423 Mabtech) overnight at 4°C. Granzyme B plates were washed 6x with 200µL PBS and blocked  
424 with RPMI 10% FBS (Gibco) ('R-10') at 37°C 5% CO<sub>2</sub>. PBMCs were thawed and resuspended in  
425 R10 and added to plates at 100,000-200,000 cells/well. HIV peptide pools (20µg/mL/peptide)  
426 were added at 10µL/well for a final concentration of 1µg/mL/peptide in <0.5% DMSO. CMV-pp65  
427 peptide pools were added at 10µL/well for a final concentration of 1µg/mL/peptide in <0.5%  
428 DMSO. PHA was dissolved in DMSO and PBS to 200µg/mL, and then added to a final

429 concentration of 1µg/mL as a positive control. 0.5% DMSO in PBS and R-10 media were used as  
430 negative controls. Plates were incubated for 18 hours at 37°C with 5% CO<sub>2</sub>. Plates were washed  
431 6x with 200µL PBS. Biotinylated secondary IFN-γ antibody (clone 7-B6-1, Mabtech) at 0.5µg/mL  
432 in PBS, or biotinylated secondary anti-granzyme B antibody (clone GB11, Mabtech) at 1.0µg/mL  
433 in PBS was added to the plates to a final volume of 100µL and incubated for 1 hour in the dark.  
434 Plates were then washed 6x with PBS and 0.5µg/mL of Streptavidin-ALP (Mabtech) was added  
435 to IFN-γ plates at 100µL/well, and 1µg/mL of Streptavidin-ALP (Mabtech) was added to granzyme  
436 B plates at 100µL/well and incubated for 1 hour. Plates were washed 6x with PBS and then color  
437 development substrate solution: 10.6mL of ddH<sub>2</sub>O, 400µL 25x AP Color Development Buffer  
438 (Biorad), 100µL AP color reagent A (Biorad), and 100µL AP color reagent B (Biorad) was added  
439 to the plate at 100µL/well for 15 minutes. After removal of the color development substrate  
440 solution, 0.5% of Tween-20 in PBS was added at 100µL/well for 10 minutes. Plates were then  
441 washed with water, and left overnight to dry. Plates were counted using Immunospot S6 Ultimate  
442 Analyzer and ImmunoSpot software (Cellular Technology Limited).

#### 443 *Statistics*

444 Statistical analyses including univariate statistics and Spearman *r* correlations and partial  
445 correlations (adjusting for potential confounders) were conducted in SAS University Edition.  
446 Slopes of change in **Fig. 4B** and **Tables S5-S6 and S9-S10** were calculated based on absolute  
447 changes on a linear scale between weeks 24-168 post-A5321 study entry, excluding participants  
448 who had a change from 0 magnitude to 0 magnitude. Analyses for **Tables S7-S8 and S11-S12**  
449 used slopes of change calculated based on proportional changes on a log<sub>10</sub> scale between weeks  
450 24-168 post-A5321 study entry, excluding participants who had a change from 0 magnitude to 0  
451 magnitude; slopes reflecting a change from 0 magnitude to a non-zero magnitude were analyzed  
452 as the highest rank, and slopes reflecting a change from a non-zero magnitude to 0 magnitude  
453 were analyzed as the lowest rank. Statistical analyses including one-way ANOVA and Wilcoxon

454 signed-rank tests were conducted in GraphPad Prism v.8.0. Plots for figures were made in  
455 GraphPad Prism v.8.0 and SAS University Edition. A custom code was generated in MATLAB  
456 v.9.7 to produce the correlogram in **Fig. 4B**. All linear mixed-effects models were conducted using  
457 the R 'lme4' package (59), with random intercepts only or both random intercepts and random  
458 slopes on the participant level modeled for the random effects, as assessed by significantly  
459 improved model fit when random slopes were included (using the R ANOVA function to compare  
460 models); multiple comparisons were made where indicated using the R 'multcomp' package (60),  
461 adjusting for multiple comparisons using Tukey's all-pair method. Linear mixed-effects models  
462 used  $\log_{10}$ -transformed response data, treating zero-valued responses as missing data.  
463 Imputation was not used to address missing data, as the degree of missingness was low. All  
464 statistical tests were two-sided,  $\alpha=0.05$ .

#### 465 *Study Approval*

466 Ethics oversight for part 1 of this study, for participants from Maple Leaf Medical Clinic, was  
467 provided by The George Washington University under IRB protocol #021750. Participants were  
468 recruited via convenience sampling by research staff at Maple Leaf Medical Clinic during routine  
469 care visits; prospective participants were provided a verbal description of the research and a copy  
470 of the informed consent form, which detailed the study's objectives, risks, and benefits. For part  
471 2 of this study, each ACTG A5321 clinical research site had the A5321 protocol and consent form,  
472 and its relevant parental protocols and consent forms, approved by their local IRB, as well as  
473 registered with and approved by the Division of AIDS (DAIDS) Regulatory Support Center (RSC)  
474 Protocol Registration Office, prior to any participant recruitment and enrollment. Once a  
475 participant for study entry was identified, details were carefully discussed with the prospective  
476 participant by clinical staff at the site. The participant (or, when necessary, the parent or legal  
477 guardian if the participant was under guardianship) was asked to read and sign the ACTG-  
478 approved protocol consent form.

479

480 **Author contributions:** RBJ designed the study. EMS, ARW, RT, AST, SHH, TRD, ST, JKB,  
481 TMM, AD, GQL, AG, PK, WDCA, JCC, and BM performed experiments. EMS, ARW, RT, ST,  
482 SHH, JKB, CML, RJB, BM, JCC, and JWM analyzed data. RTG, DKM, JJE, and JWM provided  
483 participant data. EMS, ARW, and RBJ wrote the manuscript. All authors contributed to the  
484 critical revision of the manuscript.

485

486 **Acknowledgments:** This work was supported by 1) the Martin Delaney 'BELIEVE'  
487 Collaboratory (NIH grant 1UM1AI26617), which is supported by the following NIH Co-Funding  
488 and Participating Institutes and Centers: NIAID, NCI, NICHD, NHLBI, NIDA, NIMH, NIA, FIC,  
489 and OAR; 2) by the National Institute of Allergy and Infectious Diseases of the National  
490 Institutes of Health under Award Number UM1 AI068634, UM1 AI068636 and UM1 AI106701;  
491 and 3) by a grant from the AIDS Clinical Trials Group Network (ACTG) to the University of  
492 Pittsburgh Virology Specialty Laboratory. It was also supported in part by the NIH funded R01  
493 grants AI31798 and AI147845, and by an ACTG special projects grant (to RBJ). We thank Shy  
494 Genel for assistance with MATLAB coding. We gratefully acknowledge the contributions of the  
495 study participants, without whom this work would not be possible. The content is solely the  
496 responsibility of the authors and does not necessarily represent the official views of the National  
497 Institutes of Health.

498 JWM is a consultant to Gilead Sciences and Merck, and owns share options in Co-Crystal  
499 Pharmaceuticals and Abound Bio, Inc., which are not involved in the current work. JJE has  
500 research funding outside the current work from ViiV Healthcare, Gilead Sciences and Janssen,  
501 and has consulting income from ViiV Healthcare, Gilead Sciences, Janssen, and Merck. BM has  
502 received research funding from Gilead Sciences. RTG has served on a scientific advisory board  
503 for Merck. EMS volunteers on the Board of Directors of the non-profit community clinic the

504 Berkeley Community Health Project. The authors declare that they have no other perceived  
505 conflicts of interest.

506

## 507 **References**

508 1. UNAIDS. Global HIV and AIDS statistics - 2019 fact sheet [Internet]. *FACT SHEET – WORLD*  
509 *AIDS DAY 2019*; <https://www.unaids.org/en/resources/fact-sheet>.

510 2. Andrade VM et al. A minor population of macrophage-tropic HIV-1 variants is identified in  
511 recrudescing viremia following analytic treatment interruption. *Proceedings of the National*  
512 *Academy of Sciences* 2020;117(18):9981–9990.

513 3. Ganor Y et al. HIV-1 reservoirs in urethral macrophages of patients under suppressive  
514 antiretroviral therapy. *Nature Microbiology* 2019;4(4):633–644.

515 4. Finzi D et al. Identification of a Reservoir for HIV-1 in Patients on Highly Active Antiretroviral  
516 Therapy. *Science* 1997;278(5341):1295–1300.

517 5. Chun TW et al. Presence of an inducible HIV-1 latent reservoir during highly active  
518 antiretroviral therapy. *Proceedings of the National Academy of Sciences of the United States of*  
519 *America* 1997;94(24):13193–13197.

520 6. Wong JK et al. Recovery of Replication-Competent HIV Despite Prolonged Suppression of  
521 Plasma Viremia. *Science* 1997;278(5341):1291–1295.

522 7. Siliciano JD, Siliciano RF. Enhanced Culture Assay for Detection and Quantitation of Latently  
523 Infected, Resting CD4+ T-Cells Carrying Replication-Competent Virus in HIV-1-Infected  
524 Individuals. In: *Human Retrovirus Protocols*. New Jersey: Humana Press; 2005:003–016

525 8. Siliciano JD et al. Long-term follow-up studies confirm the stability of the latent reservoir for  
526 HIV-1 in resting CD4+ T cells. *Nature Medicine* 2003;9(6):727–728.

527 9. Castagna A et al. Analytical treatment interruption in chronic HIV-1 infection: time and  
528 magnitude of viral rebound in adults with 10 years of undetectable viral load and low HIV-DNA  
529 (APACHE study). *Journal of Antimicrobial Chemotherapy* 2019;74(7):2039–2046.

530 10. Deeks SG. Shock and kill. *Nature* 2012;487(7408):439–440.

531 11. Huang S-H et al. Have Cells Harboring the HIV Reservoir Been Immunoedited?. *Frontiers in*  
532 *Immunology* 2019;10. doi:10.3389/fimmu.2019.01842

533 12. Yukl SA et al. HIV latency in isolated patient CD4 + T cells may be due to blocks in HIV  
534 transcriptional elongation, completion, and splicing. *Science Translational Medicine*  
535 2018;10(430):eaap9927.

536 13. Fischer M et al. Cellular Viral Rebound after Cessation of Potent Antiretroviral Therapy  
537 Predicted by Levels of Multiply Spliced HIV-1 RNA Encoding nef. *The Journal of Infectious*  
538 *Diseases* 2004;190(11):1979–1988.

- 539 14. Pace MJ, Agosto L, Graf EH, O'Doherty U. HIV reservoirs and latency models. *Virology*  
540 2011;411(2):344–354.
- 541 15. Cohn LB, Chomont N, Deeks SG. The Biology of the HIV-1 Latent Reservoir and  
542 Implications for Cure Strategies. *Cell Host & Microbe* 2020;27(4):519–530.
- 543 16. Mota TM et al. Integrated Assessment of Viral Transcription, Antigen Presentation, and CD8  
544 + T Cell Function Reveals Multiple Limitations of Class I-Selective Histone Deacetylase  
545 Inhibitors during HIV-1 Latency Reversal. *Journal of Virology* 2020;94(9).  
546 doi:10.1128/JVI.01845-19
- 547 17. Jones RB et al. A Subset of Latency-Reversing Agents Expose HIV-Infected Resting CD4+  
548 T-Cells to Recognition by Cytotoxic T-Lymphocytes. *PLOS Pathogens* 2016;12(4):e1005545.
- 549 18. Casazza JP, Betts MR, Picker LJ, Koup RA. Decay Kinetics of Human Immunodeficiency  
550 Virus-Specific CD8+ T Cells in Peripheral Blood after Initiation of Highly Active Antiretroviral  
551 Therapy. *Journal of Virology* 2001;75(14):6508–6516.
- 552 19. Kalams SA et al. Levels of human immunodeficiency virus type 1-specific cytotoxic T-  
553 lymphocyte effector and memory responses decline after suppression of viremia with highly  
554 active antiretroviral therapy. *Journal of Virology* 1999;73(8):6721–6728.
- 555 20. Ogg GS et al. Decay Kinetics of Human Immunodeficiency Virus-Specific Effector Cytotoxic  
556 T Lymphocytes after Combination Antiretroviral Therapy. *Journal of Virology* 1999;73(1):797–  
557 800.
- 558 21. Xu Y et al. HIV-Specific T Cell Responses Are Highly Stable on Antiretroviral Therapy.  
559 *Molecular Therapy - Methods & Clinical Development* 2019;15:9–17.
- 560 22. Rouzioux C, Avettand-Fenoël V. Total HIV DNA: a global marker of HIV persistence.  
561 *Retrovirology* 2018;15(1):30.
- 562 23. Imamichi H et al. Defective HIV-1 proviruses produce novel protein-coding RNA species in  
563 HIV-infected patients on combination antiretroviral therapy. *Proceedings of the National*  
564 *Academy of Sciences* 2016;113(31):8783–8788.
- 565 24. Wolint P, Betts MR, Koup RA, Oxenius A. Immediate Cytotoxicity But Not Degranulation  
566 Distinguishes Effector and Memory Subsets of CD8+ T Cells. *Journal of Experimental Medicine*  
567 2004;199(7):925–936.
- 568 25. Shin H, Blackburn SD, Blattman JN, Wherry EJ. Viral antigen and extensive division  
569 maintain virus-specific CD8 T cells during chronic infection. *Journal of Experimental Medicine*  
570 2007;204(4):941–949.
- 571 26. Rock MT et al. Differential Regulation of Granzyme and Perforin in Effector and Memory T  
572 Cells following Smallpox Immunization. *The Journal of Immunology* 2005;174(6):3757–3764.
- 573 27. Roberts ER et al. Collapse of Cytolytic Potential in SIV-Specific CD8+ T Cells Following  
574 Acute SIV Infection in Rhesus Macaques. *PLOS Pathogens* 2016;12(12):e1006135.

- 575 28. McElhaney JE et al. Granzyme B: Correlates with protection and enhanced CTL response to  
576 influenza vaccination in older adults. *Vaccine* 2009;27(18):2418–2425.
- 577 29. Deng K et al. Broad CTL response is required to clear latent HIV-1 due to dominance of  
578 escape mutations. *Nature* 2015;517(7534):381–385.
- 579 30. Sewell AK et al. IFN-gamma exposes a cryptic cytotoxic T lymphocyte epitope in HIV-1  
580 reverse transcriptase. *Journal of Immunology* 1999;162(12):7075–7079.
- 581 31. Gandhi RT et al. Levels of HIV-1 persistence on antiretroviral therapy are not associated  
582 with markers of inflammation or activation. *PLOS Pathogens* 2017;13(4):e1006285.
- 583 32. Thomas AS et al. T-cell responses targeting HIV Nef uniquely correlate with infected cell  
584 frequencies after long-term antiretroviral therapy. *PLOS Pathogens* 2017;13(9):e1006629.
- 585 33. Addo MM et al. Comprehensive Epitope Analysis of Human Immunodeficiency Virus Type 1  
586 (HIV-1)-Specific T-Cell Responses Directed against the Entire Expressed HIV-1 Genome  
587 Demonstrate Broadly Directed Responses, but No Correlation to Viral Load. *Journal of Virology*  
588 2003;77(3):2081–2092.
- 589 34. Nowacki TM et al. Granzyme B production distinguishes recently activated CD8+ memory  
590 cells from resting memory cells. *Cellular Immunology* 2007;247(1):36–48.
- 591 35. Migueles SA et al. Lytic Granule Loading of CD8+ T Cells Is Required for HIV-Infected Cell  
592 Elimination Associated with Immune Control. *Immunity* 2008;29(6):1009–1021.
- 593 36. Shafer-Weaver K et al. The Granzyme B ELISPOT assay: an alternative to the 51Cr-release  
594 assay for monitoring cell-mediated cytotoxicity. *Journal of Translational Medicine* 2003;1(1):14.
- 595 37. Yue FY et al. HIV-Specific Granzyme B-Secreting but Not Gamma Interferon-Secreting T  
596 Cells Are Associated with Reduced Viral Reservoirs in Early HIV Infection. *Journal of Virology*  
597 2017;91(8). doi:10.1128/JVI.02233-16
- 598 38. Pasternak AO, Berkhout B. What do we measure when we measure cell-associated HIV  
599 RNA. *Retrovirology* 2018;15(1):13.
- 600 39. Felber BK, Hadzopoulou-Cladaras M, Cladaras C, Copeland T, Pavlakis GN. Rev protein of  
601 human immunodeficiency virus type 1 affects the stability and transport of the viral mRNA.  
602 *Proceedings of the National Academy of Sciences* 1989;86(5):1495–1499.
- 603 40. Malim MH, Hauber J, Le S-Y, Maizel J v., Cullen BR. The HIV-1 rev trans-activator acts  
604 through a structured target sequence to activate nuclear export of unspliced viral mRNA. *Nature*  
605 1989;338(6212):254–257.
- 606 41. Ho Y-C et al. Replication-Competent Noninduced Proviruses in the Latent Reservoir  
607 Increase Barrier to HIV-1 Cure. *Cell* 2013;155(3):540–551.
- 608 42. Pollack RA et al. Defective HIV-1 Proviruses Are Expressed and Can Be Recognized by  
609 Cytotoxic T Lymphocytes, which Shape the Proviral Landscape. *Cell Host & Microbe*  
610 2017;21(4):494-506.e4.

- 611 43. Allen TM et al. De Novo Generation of Escape Variant-Specific CD8+ T-Cell Responses  
612 following Cytotoxic T-Lymphocyte Escape in Chronic Human Immunodeficiency Virus Type 1  
613 Infection. *Journal of Virology* 2005;79(20):12952–12960.
- 614 44. Warren J et al. HIV-1 in the latent reservoir is largely sensitive to circulating T cells. *Journal*  
615 *of Virus Eradication* 2019;5(Supplement 3):PP 5.7.9.
- 616 45. Veenhuis RT et al. Long-term remission despite clonal expansion of replication-competent  
617 HIV-1 isolates. *JCI Insight* 2018;3(18). doi:10.1172/jci.insight.122795
- 618 46. Lee GQ et al. Clonal expansion of genome-intact HIV-1 in functionally polarized Th1 CD4+  
619 T cells. *Journal of Clinical Investigation* 2017;127(7):2689–2696.
- 620 47. Cohn LB et al. HIV-1 Integration Landscape during Latent and Active Infection. *Cell*  
621 2015;160(3):420–432.
- 622 48. Wang Z et al. Expanded cellular clones carrying replication-competent HIV-1 persist, wax,  
623 and wane. *Proceedings of the National Academy of Sciences* 2018;115(11):E2575–E2584.
- 624 49. Pinzone MR et al. Longitudinal HIV sequencing reveals reservoir expression leading to  
625 decay which is obscured by clonal expansion. *Nature Communications* 2019;10(1):728.
- 626 50. Antar AA et al. Longitudinal study reveals HIV-1–infected CD4+ T cell dynamics during long-  
627 term antiretroviral therapy. *Journal of Clinical Investigation* 2020;130(7):3543–3559.
- 628 51. Knapp DJHF et al. Increasingly Successful Highly Active Antiretroviral Therapy Delays the  
629 Emergence of New HLA Class I–Associated Escape Mutations in HIV-1. *Clinical Infectious*  
630 *Diseases* 2012;54(11):1652–1659.
- 631 52. Ren Y et al. BCL-2 antagonism sensitizes cytotoxic T cell–resistant HIV reservoirs to  
632 elimination ex vivo. *Journal of Clinical Investigation* 2020;130(5):2542–2559.
- 633 53. Medema JP et al. Expression of the Serpin Serine Protease Inhibitor 6 Protects Dendritic  
634 Cells from Cytotoxic T Lymphocyte–Induced Apoptosis. *The Journal of Experimental Medicine*  
635 2001;194(5):657–668.
- 636 54. Patel SJ et al. Identification of essential genes for cancer immunotherapy. *Nature*  
637 2017;548(7669):537–542.
- 638 55. Hong F et al. Novel Assays for Measurement of Total Cell-Associated HIV-1 DNA and RNA.  
639 *Journal of Clinical Microbiology* 2016;54(4):902–911.
- 640 56. Cillo AR et al. Improved Single-Copy Assays for Quantification of Persistent HIV-1 Viremia  
641 in Patients on Suppressive Antiretroviral Therapy. *Journal of Clinical Microbiology*  
642 2014;52(11):3944–3951.
- 643 57. Laird GM, Rosenbloom DIS, Lai J, Siliciano RF, Siliciano JD. Measuring the Frequency of  
644 Latent HIV-1 in Resting CD4+ T Cells Using a Limiting Dilution Coculture Assay. In: *Methods in*  
645 *Molecular Biology*. 2016:239–253



646 58. Rosenbloom DIS et al. Designing and Interpreting Limiting Dilution Assays: General  
647 Principles and Applications to the Latent Reservoir for Human Immunodeficiency Virus-1. *Open*  
648 *Forum Infectious Diseases* 2015;2(4):ofv123.

649 59. Bates D, Mächler M, Bolker B, Walker S. Fitting Linear Mixed-Effects Models Using lme4.  
650 *Journal of Statistical Software* 2015;67(1). doi:10.18637/jss.v067.i01

651 60. Hothorn T, Bretz F, Westfall P. Simultaneous Inference in General Parametric Models.  
652 *Biometrical Journal* 2008;50(3):346–363.

653

654

655

656

657

658

659

660

661

662

663

664

665

666

667

668

669

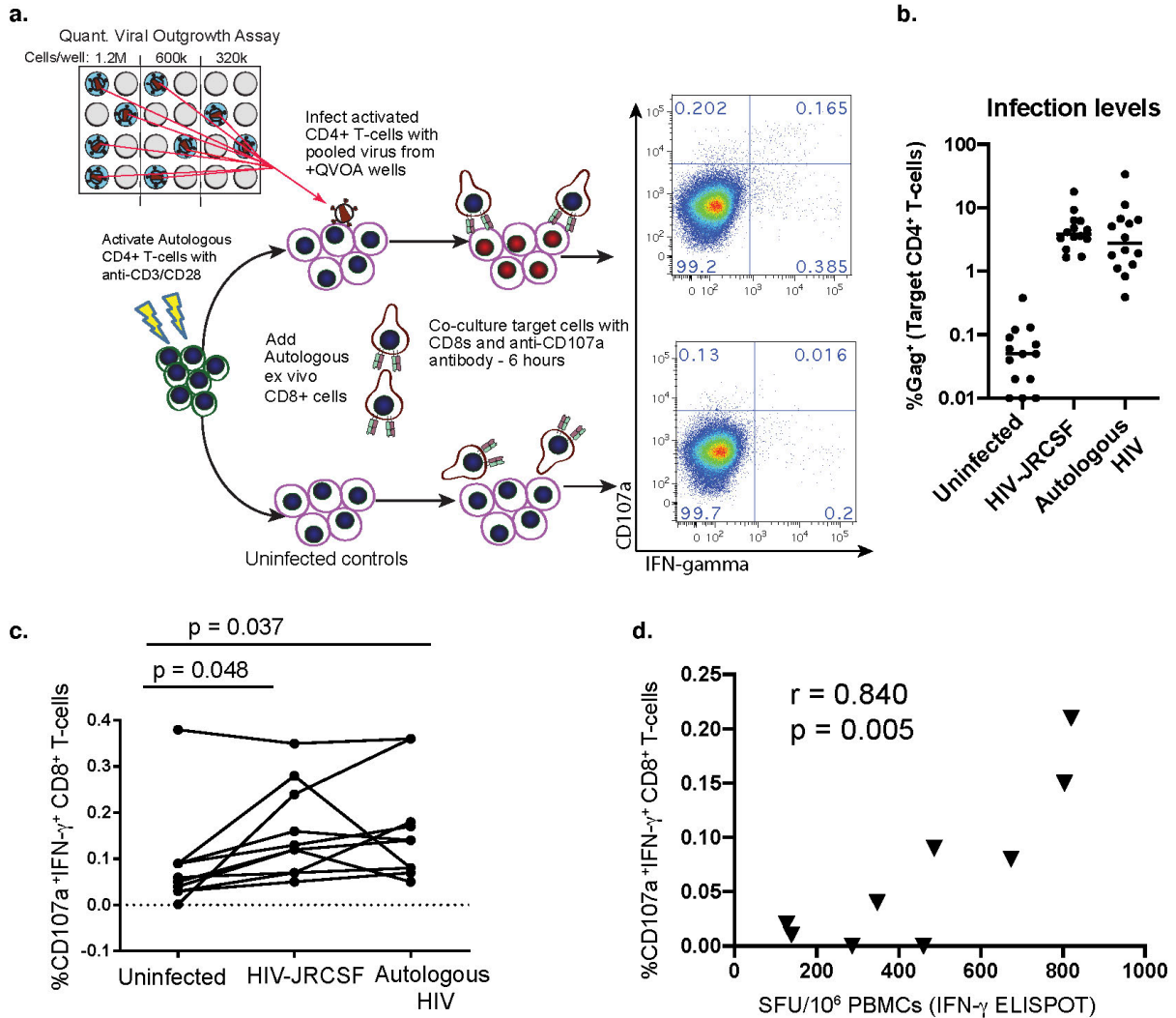
670

671

672

673

674 **Figures and figure legends**



675

676 **Fig. 1. CD8<sup>+</sup> T-cell responses to virus-infected cells can be detected ex vivo, correlating**  
 677 **with ELISPOT responses. A.** Schematic of ‘biosensor assay’. Top-right: Flow cytometry plot  
 678 gated on CD8<sup>+</sup> T-cells co-cultured with infected CD4<sup>+</sup> T-cells. Bottom-right: Uninfected control. **B.**  
 679 CD4<sup>+</sup> target cells’ infection levels from all assays, measured by flow cytometry. **C.** Flow cytometry  
 680 data depicting %CD107a<sup>+</sup>IFN- $\gamma$ <sup>+</sup> of viable CD8<sup>+</sup> T-cells, each line representing a different  
 681 participant (means from 3 replicates). P-values calculated by RM one-way ANOVA with Dunnett’s

682 multiple comparison test. **D.** Spearman's correlation between background (uninfected) subtracted  
683 responses to autologous HIV (as in **C**), and summed IFN- $\gamma$  ELISPOT responses to HIV proteome.

684

685

686

687

688

689

690

691

692

693

694

695

696

697

698

699

700

701

702

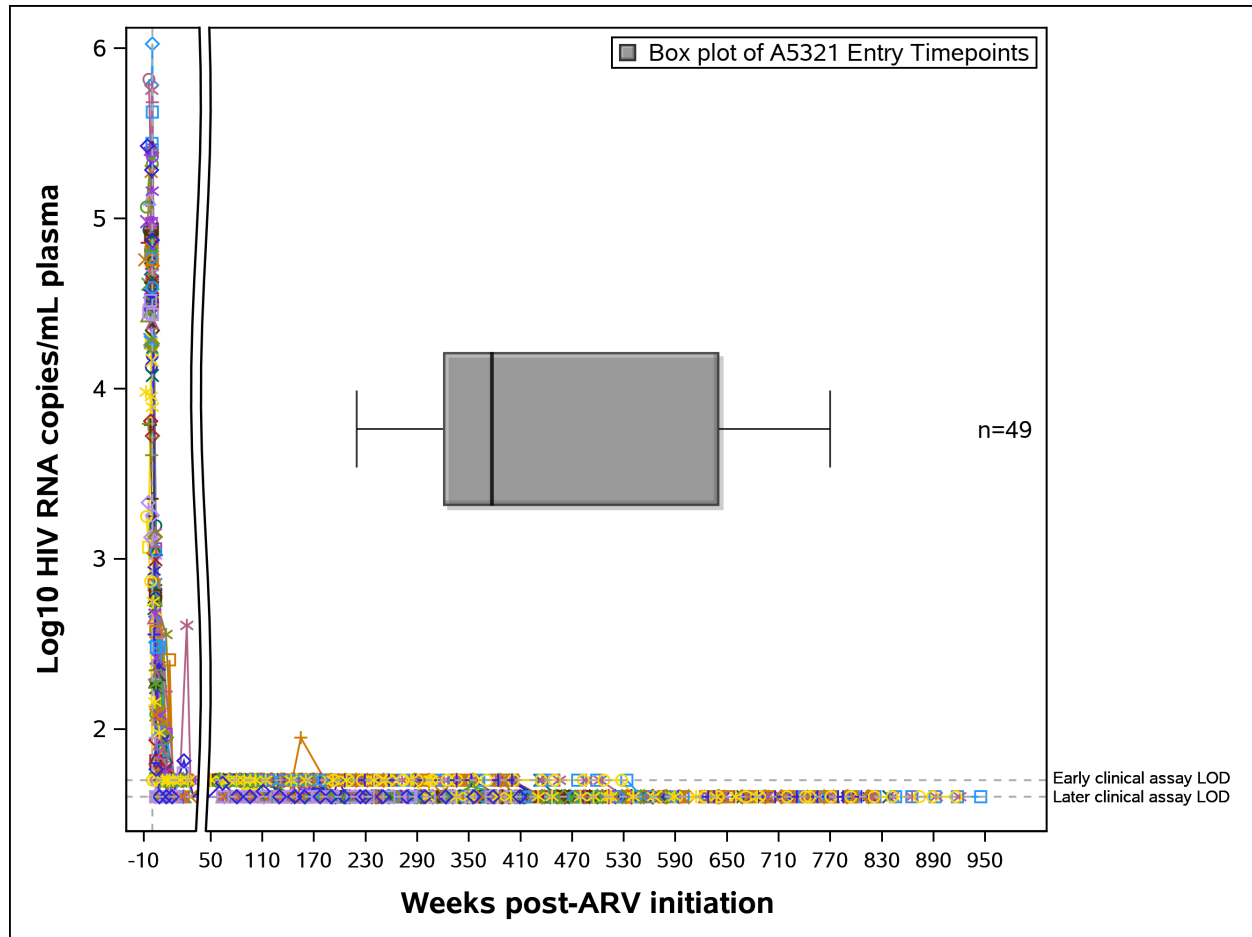
703

704

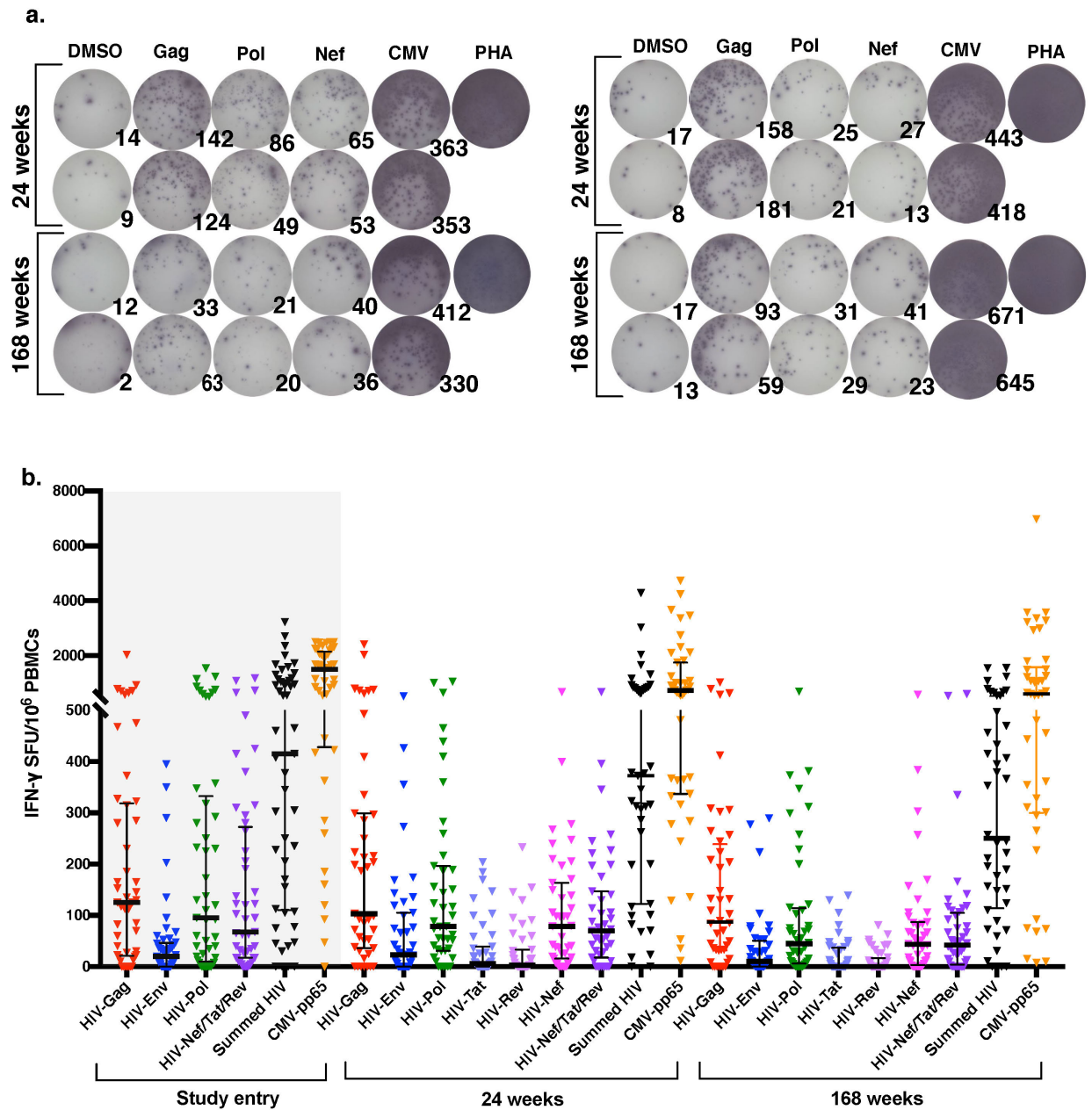
705

706

707



709 **Fig. 2. ACTG A5321 Cohort participants achieved viral suppression prior to study entry**  
710 **and maintained viral suppression throughout the study period.** Log<sub>10</sub> plasma HIV RNA  
711 (copies/mL) by clinical commercial assays for ACTG A5321 Cohort study participants included  
712 in this longitudinal sub-study, followed from pre-ART initiation (ART initiated in other ACTG  
713 trials) through to the A5321 study 168 week timepoint. Limit of detection (LOD) for early clinical  
714 assays was 50 copies/mL, and for later clinical assays 40 copies/mL. Colored lines represent  
715 individual participants (n=49), with symbols indicating each clinical viral load measurement. X-  
716 axis break shows time post-ART initiation when all participants achieved initial viral suppression.  
717 Box plot shows the distribution of participants' A5321 study entry timepoints relative to weeks  
718 post-ART initiation (minimum, Q1, median, Q3, maximum).



719

720 **Fig. 3. HIV-specific T-cell responses readily detectable ex vivo and persist on long-term**  
 721 **ART, primarily directed against HIV-Gag, HIV-Pol, and HIV-Nef. A.** Representative IFN- $\gamma$   
 722 ELISPOT results for two participants for both timepoints, with  $2 \times 10^5$  PBMCs/well. **B.** Magnitudes  
 723 of IFN- $\gamma$  responses are shown for three on-ART timepoints. Study entry timepoint data is shaded

724 in gray because it was not performed in batch with 24 and 168 weeks timepoints. Each data point  
725 represents the mean spot forming units (SFU)/10<sup>6</sup> PBMCs following background subtraction of  
726 negative control wells (duplicates). Vertical lines and error bars represent median and interquartile  
727 range for each peptide pool.

728

729

730

731

732

733

734

735

736

737

738

739

740

741

742

743

744

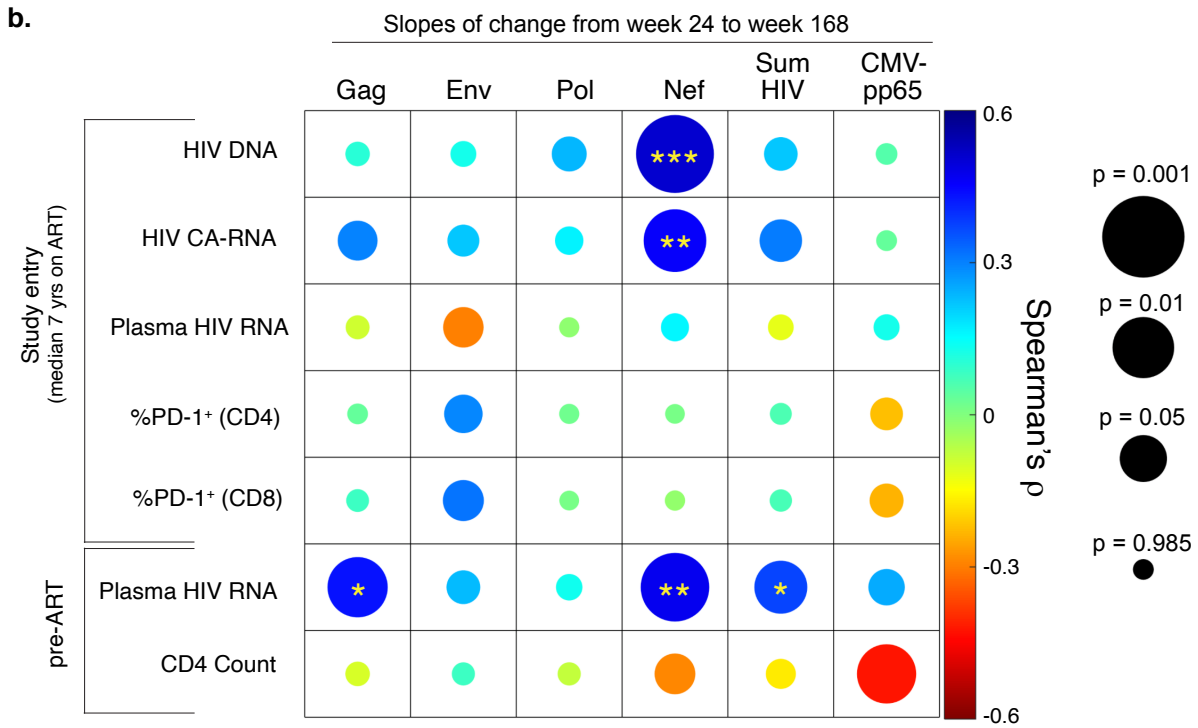
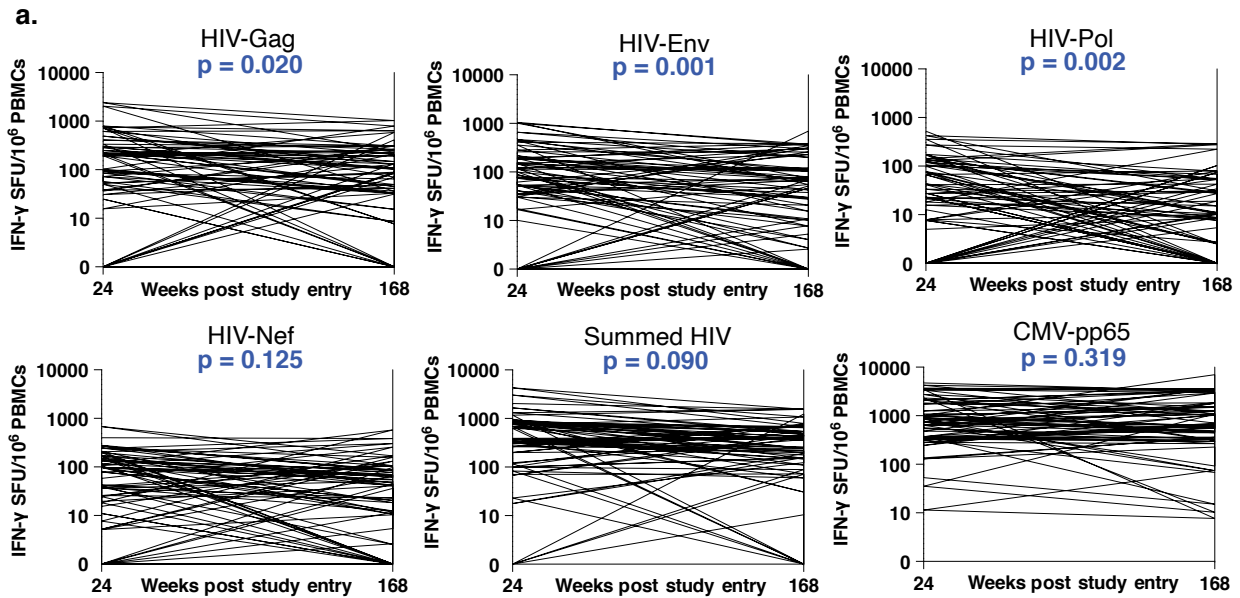
745

746

747

748

749



750

751 **Fig. 4. HIV-specific T-cell responses highly stable on long-term ART, with HIV-Nef-specific**  
 752 **response dynamics uniquely associated with reservoir measures. A.** Participant-specific  
 753 slopes of change in T-cell responses from weeks 24 to 168 post-study entry. P-values represent

754 the significance level for the covariate time (in weeks) in linear mixed-effects models from **Table**  
755 **S4. B.** Correlogram depicting Spearman correlations between slopes of change in raw  
756 magnitudes of T-cell responses (from panel **A**) with virologic and immunologic parameters. Color  
757 scale bar represents magnitude of correlation coefficient. Circle size represents unadjusted p-  
758 values. Asterisks represent adjusted p-values controlling for pre-ART plasma HIV RNA and CD4<sup>+</sup>  
759 T-cell count (\* <0.05, \*\* <0.01, \*\*\* <0.001).

760

761

762

763

764

765

766

767

768

769

770

771

772

773

774

775

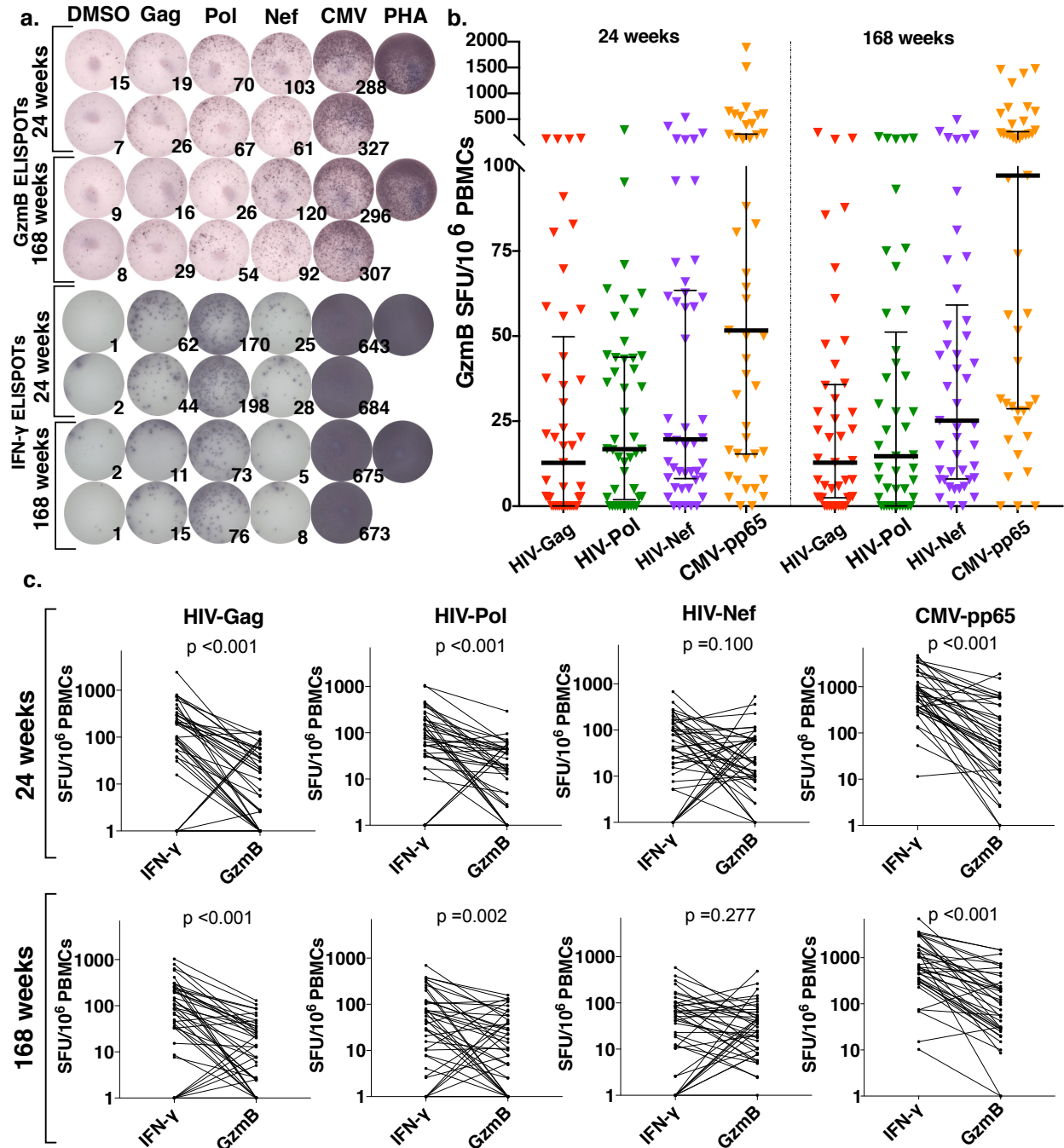
776

777

778

779





780

781 **Fig. 5. HIV-specific T-cells demonstrate cytotoxic ability, preferentially directed towards**

782 **HIV-Nef, evidencing recent *in vivo* antigen exposure. A.** Corresponding granzyme B and IFN-

783  $\gamma$  ELISPOT results for one participant at both timepoints, with  $2 \times 10^5$  PBMCs/well. **B.** Magnitudes

784 of granzyme B responses are shown for two batched on-ART timepoints. Each data point

785 represents the mean number of SFU/10<sup>6</sup> PBMCs following background subtraction of mean of

786 negative control wells. Vertical lines and error bars represent median and interquartile range for  
787 each peptide pool. **C.** Pairwise comparisons of granzyme B versus IFN- $\gamma$  responses for Gag, Pol,  
788 Nef, and CMVpp65 at both timepoints. P-values calculated by Wilcoxon matched pairs signed-  
789 rank test.

790

791

792

793

794

795

796

797

798

799

800

801

802

803

804

805

806

807

808

809

810

811 **Tables**

**Table 1. Demographic, virologic, and immunologic characteristics of longitudinal sub-study participants**

Continuous Variables	Median	Range		Missing		Categorical Variables	n	%
		Lower	Upper	n	%			
Age at A5321 entry (years)	48	23	74	0	0.00%	Sex		
Years on ART at A5321 entry	6.6	4.2	14.8	0	0.00%	Female	11	22.45%
HIV CA-DNA at A5321 entry (cps/10 <sup>6</sup> CD4+ T-cells)	515.7	5.2	5494.0	0	0.00%	Male	38	77.55%
HIV CA-RNA at A5321 entry (cps/10 <sup>6</sup> CD4+ T-cells)	24.2	13.6	898.9	2	4.08%	Race/Ethnicity		
HIV plasma RNA via iSCA at A5321 entry (cps/mL) <sup>A</sup>	0.4	0.4	8.8	3	6.12%	American Indian/Alaskan Native	1	2.04%
%PD-1+ CD4+ cells at A5321 entry	36.75%	1.20%	83.10%	5	10.20%	Black (non-Hispanic)	5	10.20%
%PD-1+ CD8+ cells at A5321 entry	35.40%	0.70%	84.90%	5	10.20%	Hispanic (regardless of Race)	16	32.65%
Pre-ART plasma HIV-1 RNA (log <sub>10</sub> cps/mL)	4.6	2.3	5.9	0	0.00%	White (non-Hispanic)	27	55.10%
Pre-ART CD4+ T-cell count (cells/mm <sup>3</sup> )	287.5	15.5	708.5	0	0.00%	iSCA qualifier at A5321 entry <sup>A</sup>		
						Undetectable	22	44.90%
						Detectable	27	55.10%

<sup>A</sup>iSCA assay limit of detection 0.4 copies HIV per mL plasma

812

813

814

815

816

817

818

819

820

821

822

823

824

825

826

827

828

829

830

831